African Journal of Microbiology Research Vol. 6(15), pp. 3673-3683, 23 April, 2012
Available online at http://www.academicjournals.org/AJMR
DOI: 10.5897/AJMR12.149
ISSN 1996-0808 ©2012 Academic Journals

Full Length Research Paper

The T3S effector XopXccN of *Xanthomonas campestris* pv. *campestris* is involved in plant defense through interference with photosystems, reactive oxygen species (ROS) generation, and callose deposition

Guo-Feng Jiang[1,2], Bo-Le Jiang[3], Li-Gang Chen[1], San Liu[3], Hong-Yu Wei[3], Wei-Jian Cen[3], Xiao-Hong Hang[3], Zong-Zhen Wen[3], Dong-Jie Tang[3], Guang-Tao Lu[3], Yong-Qiang He[3], Di-Qiu Yu[1] and Ji-Liang Tang[3]*

[1]Key Laboratory of Tropical Forest Ecology, Xishuangbanna Tropical Botanical Garden, Chinese Academy of Sciences, Kunming, Yunnan 650223, China.
[2]Graduate School of Chinese Academy of Sciences, Beijing 100049, China.
[3]State Key Laboratory for Conservation and Utilization of Subtropical Agro-bioresources, Key Laboratory of Ministry of Education for Microbial and Plant Genetic Engineering, College of Life Science and Technology, Guangxi University, Nanning, Guangxi 530004, China.

Accepted 26 March, 2012

XopXccN and XopN are important type III secreted (T3S) virulence effector proteins of *Xanthomonas campestris* pv. *campestris* (*Xcc*) and *Xanthomonas campestris* pv. *vesicatoria* (*Xcv*), respectively. They were placed in the same T3S effector class based on sequence homology. It has been demonstrated that *Xcv* XopN suppresses pathogen-associated molecular pattern-triggered immune responses during *Xcv* infection. Here, we present evidence showing that *Xcv* XopN cannot replace XopXccN for the virulence of *Xcc*. In addition, we employed two-dimensional different gel electrophoresis to investigate the differentially expressed proteins affected by *Xcc* XopXccN in the host plant Chinese radish. The results demonstrated that nine proteins mainly associated with plant photosystems were suppressed by XopXccN. RT-PCR analysis showed that several proteins were repressed by XopXccN at the transcriptional level. Moreover, XopXccN could suppress the generation of reactive oxygen species (ROS) and callose deposition in plants. Taken together, our results revealed that XopXccN is involved in plant defense through interference with photosystems, ROS generation, and callose deposition *in planta*.

Key words: XopXccN, T3S effector, *Xanthomonas campestris* pv. *campestris*, 2D-DIGE.

INTRODUCTION

It has been well-established that many *Xanthomonas* pathogens translocate the so-called effector proteins directly into plant cells via a type III secretion system (T3SS). These type III secreted (T3S) effectors are essential for the pathogens to cause disease in susceptible host plants and to elicit hypersensitive response (HR) in resistant host and non-host plants (Lindgren, 1997; Büttner and Bonas, 2006; Büttner and He, 2009). The T3S effector XopN in *Xanthomonas campestris* pathovar *vesicatoria* (*Xcv*), the causal agent of bacterial spot disease in pepper and tomato plants, has been shown to reduce pathogen-associated molecular pattern (PAMP)-induced gene expression and callose deposition in both tomato and *Arabidopsis* tissues, indicating that XopN suppresses PAMP-triggered immune

*Corresponding author. E-mail: jltang@gxu.edu.cn. Tel: 86-771-3239566. Fax: 86-771-3239413.

(PTI) responses during *Xcv* infection (Kim et al., 2008, 2009). Furthermore, it has been shown that an "LXXLL" motif in the N terminus of the XopN protein is required for tomato atypical receptor-like kinase1 (TARK1) binding and contributes to XopN-dependent virulence in tomato (Kim et al., 2009).

Xanthomonas campestris pathovar *campestris* (*Xcc*), the causal agent of black rot disease of cruciferous crops, has been used as a model bacterium for studying the molecular mechanisms of pathogen–plant interactions. In our previous work, we found that the XopN homologue XopXccN in *Xcc* is also a T3S effector, and the disruption of *xopXccN* resulted in a significant reduction in virulence and growth of the pathogen in plants (Jiang et al., 2008), indicating the importance of this effector class in bacterial pathogenesis (Roden et al., 2004; Jiang et al., 2008). However, the "LXXLL" motif is absent in *Xcc* XopXccN effector protein. Therefore, we set out to dissect the molecular mechanism of XopXccN in pathogenesis. First, we investigated whether *Xcv xopN* could replace *xopXccN* for the virulence of *Xcc*. Then, we sought the protein changes caused by XopXccN in the host plant Chinese radish. Here, we present our primary results showing that the molecular mechanism of XopXccN and XopN in pathogenesis may not be the same.

MATERIALS AND METHODS

Bacterial strains, plasmids, growth conditions, and DNA manipulations

The bacterial strains and plasmids used in this work are listed in Table 1. All *Xcc* strains were grown at 28°C in the rich medium NYG (Daniels et al., 1984). *Escherichia coli* strains were grown in LB medium (Miller, 1972) at 37°C. Antibiotics were used at the following final concentrations as required: gentamycin (Gm), 5 μg/ml; kanamycin (Kan), 25 μg/ml; rifampicin (Rif), 50 μg/ml; spectinomycin (Spc), 50 μg/ml; and tetracycline (Tc), 15 μg/ml for *E. coli* and 5 μg/ml for *Xcc* and *Xcv*. Standard DNA manipulations were performed as described by Sambrook et al. (1989). Conjugation between the *Xanthomonas* and *E. coli* strains was performed as described previously (Daniels et al., 1984). Restriction enzymes and DNA ligase were used in accordance with the manufacturer's instructions (Promega).

Construction of the *xopN* mutant and the complementary strains

To obtain the *xopN* (XCV2944) mutant, the fragment containing the integration region of *xopN* was amplified from *Xcv* 85-10 using the primer set MxopN-F/MxopN-R (Table 2) and cloned into pK18mob, generating the plasmid pKNxopN (Table 1). After confirmed by sequencing, the plasmid pKNxopN was transferred into *Xcv* 85-10 by triparental conjugation. Transconjugants were screened on NYG plates supplemented with rifampicin and kanamycin, and the obtained *xopN* mutant NKxopN (Table 1) was confirmed by PCR using the primer set PK-F/CMxopN-R (Table 2).

For construction of the complementary strain of *xopN* mutant, a 2715-bp fragment from 500-bp upstream of the start codon to 13-bp downstream of the stop codon of *xopN* was amplified from *Xcv* 85-10 using the primer set CMxopN-F/CMxopN-R (Table 2) and cloned into pK18mob, yielding pKxopN (Table 1). After confirmed by sequencing, the 2715-bp fragment was excised and cloned into pLAFR6, yielding pLxopN (Table 1). The plasmid pLxopN was transferred into *Xcv xopN* mutant NKxopN and *Xcc xopXccN* mutant 050D08 respectively by triparental conjugation, generating the complementary strains NKxopN/pLxopN and 050D08/pLxopN (Table 1).

Virulence assay

The virulence of *Xcc* and *Xcv* strains were tested using potted Chinese radish 501 by the leaf clipping method and tomato by the hand-inoculation method, respectively, as described previously (Meyer et al., 2005; Tang et al., 2005). The plants were grown in a greenhouse with a day and night cycle of 12 and 12 h with illumination via fluorescent lamp at 25 to 28°C. Bacterial cells were grown in NYG medium at 28°C with shaking at 200 rpm for 15 h. The cell concentration was adjusted to OD_{600} = 0.001 for *Xcc* clipping and 0.3 for *Xcv* infiltration. Disease symptom was measured 10 days post-inoculation. Three repeated independent experiments were performed.

Translocation assay

To detect the translocation of XopN in *Xcc*, the 1060-bp fragment containing the putative promoter and signal sequence of *xopN* (from 508-bp upstream to 552-bp downstream of the start codon) was amplified from *Xcv* 85-10 using the primer set PxopN-F/PxopN-R (Table 2) and cloned into pK18mob, yielding pKPxopN (Table 1). After confirmed by sequencing, the 1060-bp fragment was excised and cloned into pLBs1 (Xu et al., 2008), yielding pLPxopNBs1 (Table 1). The plasmid pLPxopNBs1 was introduced into the *avrBs1*-deletion mutant 8004ΔavrBs1 (Xu et al., 2008) by triparental conjugation. The obtained strain 8004ΔavrBs1/pLPxopNBs1 (Table 1) was infiltrated into leaves of pepper (*Capsicum annuum*) cv. ECW-10R. The strain 8004ΔavrBs1/pLJB0241 (Jiang et al., 2008) was used as a positive control.

Hypersensitive response test

The ability of *Xcc* strains to elicit HR was tested on pepper ECW-10R, a nonhost plant commonly used to test HR of *Xcc* (Castañeda et al., 2005; Xu et al., 2008). Bacterial cells of *Xcc* strains from overnight cultures were washed, resuspended in 10 mM sodium phosphate buffer to a concentration of OD_{600} = 0.3, and infiltrated into pepper leaf tissues using a needleless syringe. After inoculation, the plants were maintained in a greenhouse with a day/night cycle of 16/8 h illumination by fluorescent lamps and at a constant temperature of 28°C with 80% relative humidity. HR symptoms were photographed 8 h post-inoculation. At least three plants were inoculated in each experiment, and each experiment was repeated at least three times.

Protein extraction

The Chinese radish 501 leaves inoculated via mesophyll infiltration 3 days post-inoculation were ground to a powder in liquid nitrogen and extracted with phenol extraction buffer (3 ml/g fresh weight of leaves) as described previously (Isaacson et al., 2006). After 0.1 M ammonium acetate precipitation, methanol wash and acetone wash, the purified total proteins were resolved with the isoelectric focusing (IEF) buffer according to Ettan DIGE System User Manual (GE Healthcare). Proteins were further purified by 2-D Clean-Up Kit

Table 1. Bacterial strains and plasmids used in this work.

Strains or plasmids	Relevant characteristic	Source
***Xcc* and *Xcv* strains**		
Xcc 8004	Wild type, Rif^r	(Daniels et al.,1984)
Xcv 85-10	Wild type, Rif^r	Our lab's collection
050D08	*xopXccN* Tn5gusA5 insertion mutant of 8004, Rif^r, Kan^r, Gm^r, Spc^r	Our lab's collection
C050D08	050D08 harboring pLxopXccN, Rif^r, Kan^r, Tc^r	(Jiang et al., 2008)
050D08/pLxopN	050D08 harboring pLxopN, Rif^r, Kan^r, Tc^r	This work
8004ΔavrBs1	*avrBs1* deletion mutant of 8004, Rif^r, Gm^r	(Xu et al., 2008)
8004ΔavrBs1/pLPxopNBs1	8004ΔavrBs1 harboring pLPxopNBs1, Rif^r, Gm^r, Tc^r	This work
8004ΔavrBs1/pLJB0241	8004ΔavrBs1 harboring pLJB0241, Rif^r, Gm^r, Tc^r	(Jiang et al., 2008)
85-10/pLAFR6	85-10 harboring pLAFR6, Rif^r, Tc^r	This work
NKxopN	*xopN* (XCV2944) integration mutant of *Xcv* 85-10, Rif^r, Kan^r	This work
NKxopN/pLxopN	NKxopN harboring pLxopN, Rif^r, Kan^r, Tc^r	This work
NKxopN/pLAFR6	NKxopN harboring pLAFR6, Rif^r, Kan^r, Tc^r	This work
NK1553	$avrAC_{Xcc8004}$ integration mutant of 8004, Rif^r, Kan^r	(Xu et al., 2008)
Plasmids		
pK18mob	Cloning vector; Kan^r	Our lab's collection
pLAFR6	Broad host range IncP cloning cosmid, Tc^r	Our lab's collection
pKxopN	pK18mob containing the entire *xopN*, Kan^r	This work
pLxopN	pLAFR6 containing the entire *xopN*, Tc^r	This work
pKNxopN	pK18mob containing the integration region of *xopN*, Kan^r	This work
pKPxopN	pK18mob containing the promoter and signal region of *xopN*, Kan^r	This work
pLBs1	pLAFR6 containing $avrBs1_{59\text{-}445}$, Tc^r	(Xu et al., 2008)
pLPxopNBs1	pLBs1 containing the promoter and signal region of *xopN*, Tc^r	This work

and quantified using the 2D-QUANT kit (GE Healthcare). The aliquots were stored at -80°C.

Fluorescence labeling with CyDyes

The pH of protein samples were adjusted to 8.5 with 50 mM sodium hydroxide and labelled with the CyDye DIGE Fluor minimal for two-dimensional difference gel electrophoresis (2D-DIGE) technology (GE Healthcare) according to the manufacturer's recommended protocol. Three group samples were labeled with Cy3 (Chinese radish challenged with *Xcc* 8004 in gel 1 and 3 while mutant 050D08 challenged in gel 2) or Cy5 (*Xcc* 8004 challenged in gel 2 while 050D08 challenged in gel 1 and 3). Meanwhile, a mixture of equal amounts of the samples from *Xcc* 8004 challenged and 050D08 challenged were labeled with Cy2 as internal standards. In each sample 50 μg proteins were labelled with 400 pmol fluorochromes. Labeling reaction was performed and the rehydration buffer was supplemented to the labeled samples for an ultimate 450 μl volume according to Ettan DIGE System User Manual (GE Healthcare).

Difference gel electrophoresis (2D-DIGE)

The first dimension IEF was carried out by an Ettan IPG Phor system on a 24 cm DryStrip gel (non-linear pI 3 to 10, GE Healthcare) according the program: 200 V for 1 h, 500 V for 1 h, 1000 V for 1 h, 8000 V for 1 h, and 8000 V for 7 h in 20°C. Focused IEF strips were equilibrated in DTT buffer for 15 min and then placed in iodoacetamide buffer for 15 min according to Ettan DIGE System User Manual (GE Healthcare). Acrylamide gels were prepared (12.5%) and run at 25°C, 20 W per gel for approximately 6 h (Ettan DALTtwelve system, GE Healthcare). Three sets of 2D-DIGE gels for each treatment were run simultaneously to reduce the variation.

Image analysis and protein identification

The gels were scanned using a Typhoon 9410 variable mode imager (GE Healthcare) in corresponding wavelengths. After images scanning, spot fluorescence intensities were then analyzed with DeCyder 2D 6.0 software (GE Healthcare). Co-detection and quantification in differential in-gel analysis module were first used to analyze the three gels. Then, differential protein expression levels between the experimental samples were analyzed in biological variation analysis module. Protein spots that were differentially expressed in *Xcc* 8004 challenged and mutant 050D08 challenged were marked from the three gels (ratio > 1.8, $P < 0.01$).

Spots for mass spectrometric analysis were picked from a separate preparative gel on which 400 μg sample proteins challenged with mutant 050D08 had been run and stained with Coomassie G250. Protein spots indicated by 2D-DIGE analysis were excised manually, and proteins within the gel-excised spots were purified and digested to peptides for mass spectrometric analysis using a MALDI-TOF/TOF mass spectrometer 4800 Proteomics Analyzer (Applied Biosystems). Fragmentation data were queried in the National Center for Biotechnology Information non-redundant (NCBInr) database using the Mascot search engine

Table 2. Primers used in this work.

Primer name	Primer sequence	Product length (bp)
	For cloning	
MxopN-F	GGGGAATTC AAGTCATCCGCATCCGTCGATTC	300
MxopN-R	GGGGGATCC ATTGTCCGAAGCCAACTGCTG	
PK-F	GTTTTCCCAGTCACGAC	2912
CMxopN-R	AATGGATCC CCGGATCATCACCTCACACC	
CMxopN-F	AGGGAATTC CACAGATTTTTCGGCACCTCAGG	2715
CMxopN-R	AATGGATCC CCGGATCATCACCTCACACC	
PxopN-F	GGGGAATTC GTGGTGGCCACAGATTTTTCG	1060
PxopN-R	GGGGGATCC GACATTGGTGAGGAAGCTGCC	
	For qReal-time PCR	
LHCA1-F	GGCTATGCTCGCTGTTCCTG	251
LHCA1-R	ATCCAAGAGGGTCAAATGCG	
LHCA2-F	GTCGTTGAGCTCATCTTAATAGGATGGGCC	123
LHCA2-R	TCCAACGTCTGTGCCCGTCA	
Vacuolar Invertase-F	ACGACTGGTACGCGCTCGGG	129
Vacuolar Invertase-R	CGTAGAAGGTCTTGGACGCG	
RPS1-F	CAGATATCGCAACTGTTCTTCAGCCTGG	165
RPS1-R	CCATCTCCTCAGCCTTCTCG	
RuBisCO-F	TAATGGCCTACTTCTTCACATCCACCGC	134
RuBisCO-R	CGGTCCCGGAGTGAATATGA	
PsbP-F	TGACTGAGTTTATGTCCACTAGACTCGGGG	186
PsbP-R	GCCGGTTCCATTCCAAACGA	
Actin-F	GAGCGTGGTTACTCGTTCA	98
Actin-R	CTAATATCCACGTCACATTTCAT	

(http://www.matrixscience.com). Probability-based Mascot scores were used to evaluate the identifications, and only matches with $P < 0.05$ for random occurrence were considered significant.

Real-time polymerase chain reaction (RT-PCR)

The leaves of Chinese radish 501 inoculated with *Xcc* 8004, the *xopXccN* mutant 050D08, and the mutant NK1553 of $avrAC_{Xcc8004}$ (Xu et al., 2008) via mesophyll infiltration 3 days post-inoculation were ground to a powder in liquid nitrogen. Total RNA was isolated from plant tissues using TRIzol reagent (Invitrogen). For cDNA production, 1.5 µg of total RNA was reverse-transcribed using oligo(dT) 18 primer in a 20 µl reaction mixture (RevertAid First Strand cDNA Synthesis Kit, Fermentas). This template was diluted to a final concentration of 5 ng/µl and 2 µl aliquot was used for RT-PCR analysis. Actin (ACT2, AT3G18780) was used as a control in RT-PCR. The primer sets of LHCA1, LHCA2, vacuolar invertase, RPS1, RuBisCO, PsbP, and Actin were listed in Table 2.

Detection of reactive oxygen species (ROS)

Detection of ROS in leaves was performed as described by Shin and and Schachtman (2004). The leaves of Chinese radish 501 were hand-infiltrated with a 3×10^8 cells/ml suspension of *Xcc* 8004, *xopXccN* mutant 050D08, and the complementary strain C050D08. The leaves were stained with CM-H_2DCF diacetate, acetyl ester 24 h post-inoculation and then visualized using confocal microscopy (Zeiss) at 488 nm, at magnification × 200. The fluorescence intensity was quantified by the Zeiss LSM software. Eight views per sample were counted, and approximately 20 leaf guard cells were analyzed.

Callose staining

Chinese radish 501 leaves were infiltrated with a 2×10^8 cells/ml suspension of *Xcc* 8004, *xopXccN* mutant 050D08, and the complementary strain C050D08. The leaves were harvested 12 h

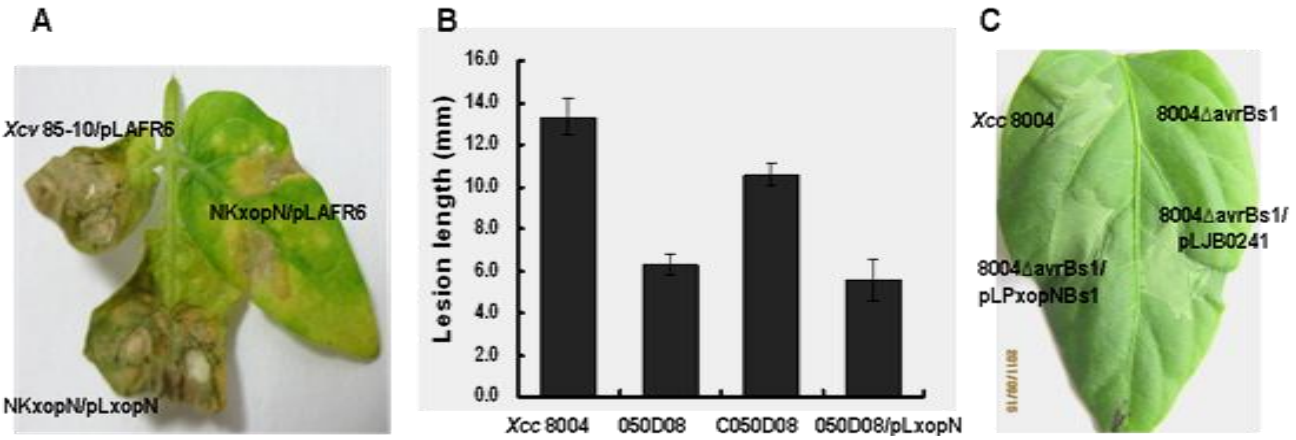

Figure 1. The complementation of *xopN* in trans and translocation of XopN. **A,** Phenotype of tomato leaves inoculated with the strains *Xcv* 85-10/pLAFR6, NKxopN/pLAFR6, and NKxopN/pLxopN. Leaves were photographed 10 days post-inoculation. Similar phenotypes were observed in at least two independent experiments. **B,** *Xcv xopN* failed to restore the reduced virulence of *Xcc xopXccN* mutant *in planta*. The Leaves of Chinese radish (*Raphanus sativus* var. *radiculus*) cv. 501 were inoculated by the leaf clipping method. The average lesion lengths caused by *Xcc* 8004, *xopXccN* mutant 050D08, the complementary strain C050D08, and the strain 050D08/pLxopN were measured 10 days post-inoculation. Values are mean ± standard deviation (SD) from three repeats, each with 30 leaves. **C,** XopN could be translocated into plant cells by *Xcc*. Bacterial cells of *Xcc* strains from overnight cultures were washed, resuspended in 10 mM sodium phosphate buffer to a concentration of OD_{600} = 0.3 and were infiltrated into pepper leaf tissues using a needleless syringe. After inoculation, the plants were maintained in a greenhouse with a day/night cycle of 16/8 h illumination by fluorescent lamps and a constant temperature of 28°C with 80% relative humidity. HR symptoms in pepper (*Capsicum annuum*) cv. ECW-10R were photographed 8 h post-inoculation. At least three plants were inoculated in each experiment, and each experiment was repeated at least three times.

after bacterial infiltration, cleared, and stained with aniline blue for callose, as described previously (Keshavarzi et al., 2004). The leaves were examined using an Axiophot D-7082 photomicroscope (Zeiss) with an A3 fluorescence cube. The number of callose depositions was determined using Image-Pro Plus software (Media Cybernetics). At least 10 adjacent view fields from each leaf (without the main vein or leaf edge) were investigated, counted and averaged.

RESULTS

Xcv xopN failed to restore the reduced virulence of *Xcc xopXccN* mutant *in planta*

According to the report of Kim and associates, the“LXXLL” motif in the N terminus of *Xcv* XopN (XCV2944, GenBank accession number YP_364675) isrequired for TARK1 binding and contributes to XopN-dependent virulence in tomato (Kim et al., 2009). Our previous work demonstrated that the disruption of *xopXccN* (XC0241, GenBank accession number YP_241348), the *xopN* homolog in *Xcc*, resulted in a significant reduction in virulence and growth of the pathogen *in planta* (Jiang et al., 2008). However, bioinformatics analysis showed that the “LXXLL” motif is absent in XopXccN, and XopXccN shares 62% identifies with XopN, while the N-terminus of XopXccN containing the putative secretion and translocation signal is distinctly different from the corresponding region of XopN. To investigate whether XopXccN has similar functionality as XopN, we determined whether the reduced virulence of the *xopXccN* mutant could be restored by *xopN* in trans. The plasmid pLxopN harboring the entire *Xcv xopN* gene was transfer into the *xopXccN* mutant 050D08 of *Xcc* and the *xopN* mutant NKxopN of *Xcv* respectively (see MATERIALS AND METHODS for details). The complementary strain C050D08 (Table 1), which contains the recombinant plasmid pLxopXccN harboring the entire *xopXccN* gene, was used as a positive control. Plant assay showed that the *Xcv xopN* mutant NKxopN caused a distinctly reduced virulence on tomato as compared to the wild type strain *Xcv* 85-10, and its reduced virulence could be restored by pLxopN in trans (Figure 1A), indicating that the plasmid pLxopN worked well. However, the virulence on Chinese radish 501 caused by 050D08/pLxopN was not significantly different with that caused by 050D08, but significantly weaker than that caused by the wild type strain 8004 and the complementary strain C050D08 (Figure 1B) ($P < 0.01$ by *t*-test). These results reveal that the reduced virulence of *Xcc xopXccN* mutant cannot be restored by the *xopN* gene of *Xcv* in trans, in other words, *Xcv xopN* cannot replace *xopXccN* for the virulence of *Xcc*.

Xcv XopN in *Xcc* could be translocated into plant cells

As described above, bioinformatics analysis revealed that the secretion and translocation signal-containing

N-termini of *Xcc* XopXccN and *Xcv* XopN are distinctly different. To verify whether *Xcv* XopN in *Xcc* can be secreted and translocated into plant cells, we employed the previously established translocation assay using the HR-inducing domain of the avirulence (Avr) effector protein AvrBs1 from *Xcc* as a reporter (Xu et al., 2008; Jiang et al., 2008, 2009). The recombinant plasmid pLPxopNBs1 (Table 1) was constructed, which contains the secretion and translocation signal domain of *Xcv* XopN fused in frame to the truncated version of *Xcc* Avr protein AvrBs1 lacking its secretion and translocation signal domain (58 N-terminal amino acids) (see MATERIALS AND METHODS for details). The plasmid pLPxopNBs1 was introduced into *Xcc avrBs1*-deletion mutant 8004ΔavrBs1 (Table 1), and the obtained strain named 8004ΔavrBs1/pLPxopNBs1 was then infiltrated into the leaves of pepper ECW-10R for HR detection. The strain 8004ΔavrBs1/pLJB0241 (Table 1) containing the T3S signal of XopXccN fused to $AvrBs1_{59-445}$ was used as a positive control. As shown in Figure 1C, the strain 8004ΔavrBs1/pLPxopNBs1 induced an obvious HR in pepper ECW-10R, the same as that induced by 8004ΔavrBs1/pLJB0241, indicating that *Xcv* XopN in *Xcc* could be secreted and translocated into plant cells.

The expression of several host proteins were suppressed by XopXccN

In order to get a clue about the function of XopXccN in host plant, we performed a 2D-DIGE to analyze the proteins differentially expressed in the *xopXccN* mutant-infected and the wild type-infected host tissues. The total protein of Chinese radish 501 leaves challenged with the wild type strain 8004 and the *xopXccN* mutant 050D08 respectively were extracted, labeled, and analyzed by 2D-DIGE (details are shown in MATERIALS AND METHODS). The three gel images in which Cy2, Cy3, and Cy5 information were collected using Typhoon 9410 variable mode imager were analyzed by DeCyder 6.0 software. A typical 2-DE gel illustrating the protein spot resolution is presented in Figure 2A, in which the Cy3, Cy5, and Cy2 labeled proteins from Chinese radish 501 challenged with strain 8004 and mutant 050D08 are shown in green, red, and blue, respectively. To sum up, 2650 global protein spots (increased 10, decreased 2, and no change 2638) (data not shown) were detected according to the condition: ratio > 1.8, $P < 0.05$ (Figure 2A). Ten differentially up-regulated protein spots (spots 966, 1931, 1998, 2001, 2007, 2012, 2032, 2087, 2389, and 2589) were observed in the mutant challenged sample (Figures 2B and C), suggesting that XopXccN might suppress the expression of these proteins in host cells. These protein spots were further identified by MALDI-TOF/TOF mass spectrometer. The fragmentation data were queried in the National Center for Biotechnology Information non-redundant (NCBInr) database (see details in MATERIALS AND METHODS). All these protein spots except one (the spot 2589) were identified (Table 3). The identified proteins show homologous to a component of the light harvesting complex (LHCA) associated with photosystem I (PSI) and photosystem II (PSII), a protein-coding PSII reaction center PsbP family protein, a large subunit of Ribulose-1,5-bisphosphate carboxylase oxygenase (RuBisCO), a vacuolar invertase, and a Ribosomal protein S1 (RPS1), respectively (Table 3). Five of them were identified as LHCA proteins (Table 3).

Some of the XopXccN-suppressed proteins are at the transcription level

To investigate whether the above differentially expressed proteins are specifically suppressed by XopXccN, and whether the expression of the proteins is repressed at the transcription level, we determined the expression of the genes encoding the proteins by RT-PCR. $AvrAC_{Xcc8004}$, another identified T3S effector in *Xcc* (Xu et al., 2008), was used as a reference. The RNA samples from the leaves of Chinese radish 501 inoculated with the wild type 8004, the *xopXccN* mutant 050D08, and the $avrAC_{Xcc8004}$ mutant NK1553 (Table 1), respectively, were surveyed. The results indicated that at the transcription level, LHCA2 and RuBisCO were specifically suppressed by XopXccN, LHCA1 and PsbP were repressed by both XopXccN and $AvrAC_{Xcc8004}$, while no obvious suppression to RPS1 and vacuolar invertase were detected (Figure 3).

XopXccN suppressed the generation of reactive oxygen species *in planta*

Since the above proteins identified by the 2D-DIGE analysis are mostly involved in plant photosystems which are the energy center associated with plant defense to phytopathogen (Zou et al., 2005; Jones et al., 2006; Yi et al., 2009; Farinati et al., 2011), it is necessary to get a further biochemical and genetic verification. The reactive oxygen species (ROS) can modulate calcium signaling in plants and is associated with plant defense using the peroxisome as an important source (Price et al., 1994; Corpas et al., 2001). ROS has a very important role in the regulation of stomatal movement in abscisic acid (ABA) signaling in guard cells, and stomata-based defense is an integral part of PAMP-triggered immunity (Melotto et al., 2008; Jannat et al., 2011). Herein, we detected the ROS in the Chinese radish 501 leaves challenged with the wild type 8004, the *xopXccN* mutant 050D08, and the complementary strain C050D08. As shown in Figure 4A, in the green fluorescence view, weaker fluorescence was detected in the guard cells in the Chinese radish 501 leaves inoculated with 8004 and C050D08, while stronger fluorescence was observed upon infection with the *xopXccN* mutant 050D08. The fluorescence intensity in Chinese radish inoculated with the mutant 050D08 were

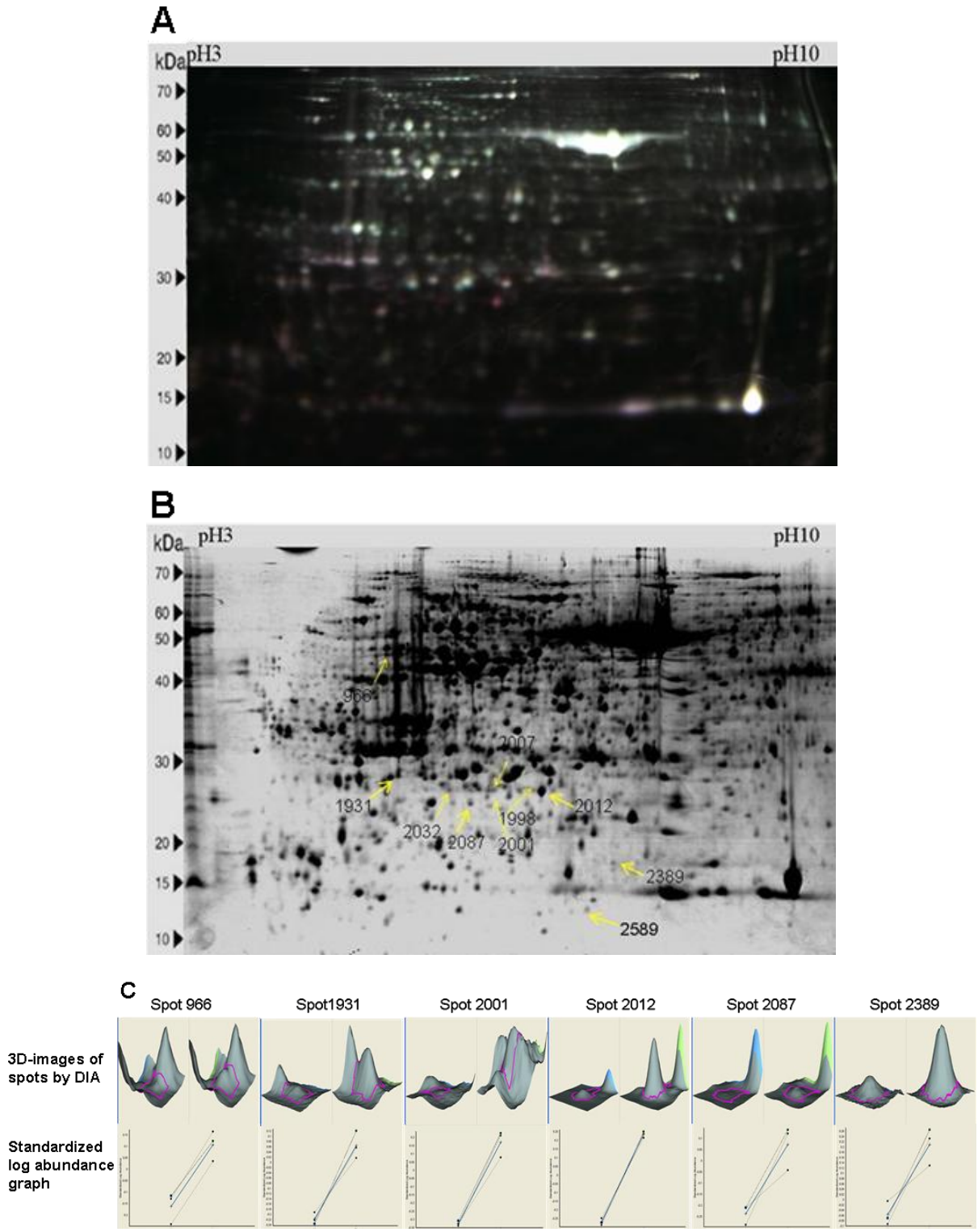

Figure 2. 2D images and differentially expressed protein spots pictures of DeCyder software analysis. **A,** 2D-DIGE image. The Cy3, Cy5, and Cy2 labeled proteins from Chinese radish (*Raphanus sativus* var. *radiculus*) cv. 501 challenged by *Xcc* 8004 and the *xopXccN* mutant 050D08 are shown in green, red, and blue, respectively. **B,** Analytical 2D gel image. The yellow arrows represent 9 gene products that are up-induced in the plant sample challenged by mutant 050D08. **C,** 3D pictures for 6 protein spots across the different samples. Here, the spots 1998, 2007, and 2032 representing the same protein LHCA1 as spot 2001 were not shown. The solid blue lines in the standardized log abundance graph represent the average protein abundance change in the different samples **C,** control group, Chinese radish challenged with *Xcc* 8004; **T**, treated group, Chinese radish challenged with the mutant 050D08). The *t*-test was used for statistical analysis using Decyder biological variation analysis software.

Table 3. Summary of the proteins suppressed by XopXccN in Chinese radish (*Raphanus sativus* var. *radiculus*) cv. 501.

Spot No.	GenBank accession No.	Protein description	Total peptides	Coverage (%)	*t*-test	Average ratio
966	gi|30692346	RPS1 protein	24	34	8.00E-03	1.86
1931	gi|145688411	LHCA2 protein	9	29	1.10E-03	1.92
1998	gi|145332845	LHCA1 protein	12	21	8.70E-07	3.27
2001	gi|145332845	LHCA1 protein	13	21	4.90E-04	3.18
2007	gi|145332845	LHCA1 protein	12	21	4.60E-04	2.29
2012	gi|79325123	PSII reaction center PsbP family protein	16	35	5.30E-06	3.19
2032	gi|13265501	LHCA1 protein	11	12	8.00E-03	2.07
2087	gi|30143305	Large subunit of RuBisCO	14	26	1.30E-02	1.82
2389	gi|46358940	Vacuolar invertase	18	21	5.50E-03	1.85

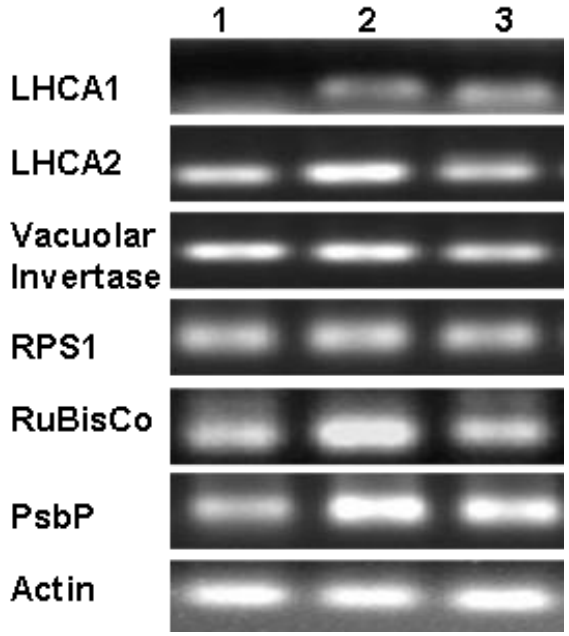

Figure 3. RT-PCR verification of differently expressed genes in Chinese radish (*Raphanus sativus* var. *radiculus*) cv. 501 challenged with *Xcc* strains 8004, 050D08, and NK1553 (Lanes 1 to 3 respectively). Two independent experiments were performed, and similar phenotypes were observed.

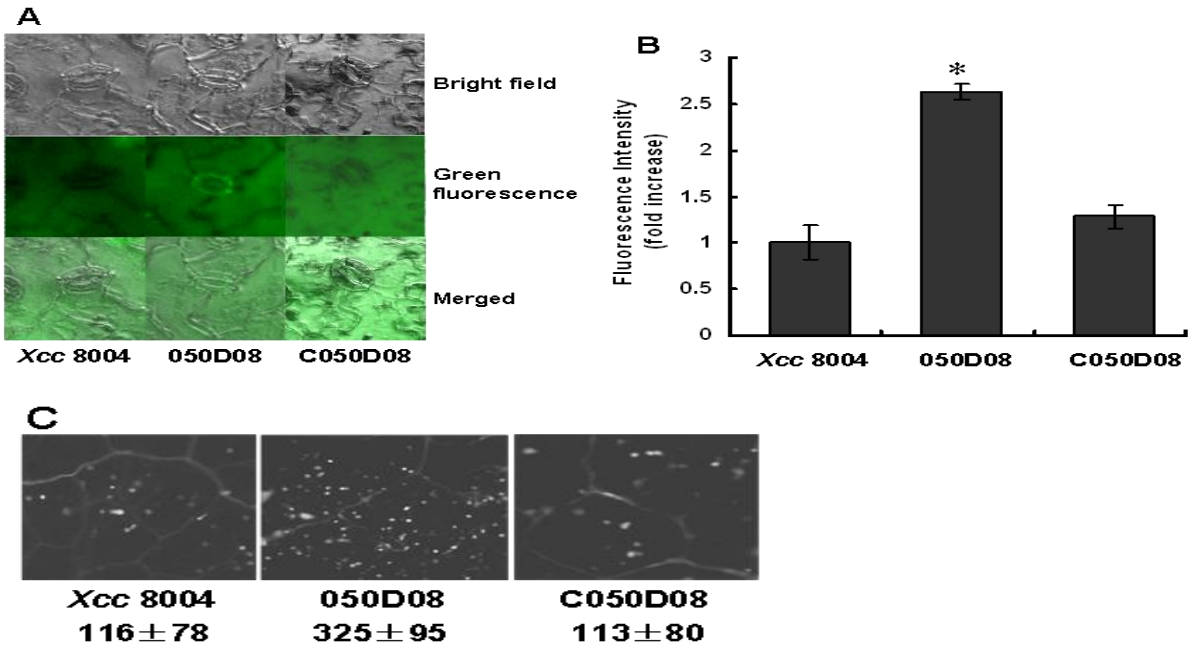

Figure 4. ROS production and callose deposition in Chinese radish (*Raphanus sativus* var. *radiculus*) cv. 501 leaves infected with *Xcc* strains. A, Detection of ROS. The leaves hand-infiltrated with *Xcc* 8004, *xopXccN* mutant 050D08, and the complementary strain C050D08 were stained 24 h post-inoculation and then visualized using confocal microscopy at 488 nm, at magnification × 200. B, Quantification of ROS. The fluorescence intensity from approximately 20 random guard cells of 8 views was quantified by the Zeiss LSM software. The fluorescence for each sample was normalized to the level observed in control cells. *means there is a significant difference when compared with the control, $P < 0.01$. Two independent experiments were performed, and similar phenotypes were observed. C, Callose deposition. Leaves were hand-infiltrated with a 2×10^8 cells/ml suspension of *Xcc* wild type strain 8004, *xopXccN* mutant 050D08, the complementary strain C050D08 and sterile water. Leaves were stained for callose after 12 h post-inoculation and then visualized using fluorescence microscopy. Values are the mean number of callose deposits ± standard deviation (SD) from five leaves from five plants. At least three independent experiments were performed, and similar phenotypes were observed.

about 2.6 folds higher than that inoculated with the wild type 8004, as indicated by the results of fluorescence quantification assay (Figure 4B, $P < 0.01$). These data reveal that XopXccN suppressed the generation of ROS *in planta*. However, no obvious difference in stomatal movement was observed.

XopXccN suppressed callose deposition *in planta*

It has been demonstrated that callose deposition, a cell wall–based defense triggered in response to PAMPs in infected host plant, is involved in the plant resistance response (DebRoy et al., 2004), and the XopN of *Xcv* suppresses callose deposition in host tissues (Kim et al., 2009). Although XopXccN lacks the “LXXLL” motif in XopN, the 2D-DIGE analysis revealed that XopXccN suppresses the expression of several proteins involved in plant photosystems that are related to plant defense. Whether XopXccN is involved in plant callose deposition should be studied. As shown in Figure 4C, callose deposition was strongly suppressed in the Chinese radish 501 leaves infected with the wild type 8004 (116±78 per mm^2) and the complementary strain C050D08 (113±80 per mm^2), as compared with the infection by the *xopXccN* mutant 050D08 (325 ± 95 per mm^2). These data suggest that XopXccN suppresses callose deposition in Chinese radish 501.

DISCUSSION

As described above, XopXccN and XopN are important T3S virulence effectors of *Xcc* and *Xcv*. According to sequence homology, these effectors have been divided into the same class that is widely conserved among *Xanthomonas* species (Roden et al., 2004). In this work we show that the XopN of *Xcv* cannot replace XopXccN for the virulence of *Xcc*, although *Xcv* XopN in *Xcc* can be secreted and translocated into host plant cells. Sequence comparison (Vector NTI Suite 9.0/AlignX) showed that *Xcc* XopXccN and *Xcv* XopN shares 72 and 62% amino acid similarity and identity, respectively. The core region from the 82nd to 676th amino acid residues of XopXccN is highly conserved to that of XopN. Like *Xcv* XopN, a three-dimensional position-specific scoring

matrix (3D-PSSM) analysis (www.sbg.bio.ic.ac.uk/~3dpssm) (Kelley et al., 2000) showed that the structure of XopXccN also contains antiparallel, α-helical tandem repeats. However, the N-terminal and C-terminal domains of XopXccN share low similarity less than 22% identity with the corresponding domain of XopN, and compared with XopN, XopXccN lacks 22 amino acid residues in the C-terminus (data not shown). How these differences in the structure of XopXccN and XopN affect the pathogenicity of *Xcc* and *Xcv* needs to be further studied.

In this work we show that *Xcc* XopXccN similar to *Xcv* XopN can also suppress callose deposition in infected host tissues. Deposition of callose at the cell wall of infected tissues is a plant defense response to pathogens. This suggests that like *Xcv* XopN, *Xcc* XopXccN also suppresses host cell wall–based defense. In addition, Mass spectrometry results from 2D-DIGE analysis and the RT-PCR results show that XopXccN interferes with the photosystem-related proteins in Chinese radish 501, i.e., five LHCA proteins, PsbP, and RuBisCO (Table 3, Figures 2 and 3). It is known that plant photosystems are the energy center associated with plant defense to phytopathogens (Zou et al., 2005; Jones et al., 2006; Yi et al., 2009; Farinati et al., 2011). Two photosystems, photosystem I (PSI) and photosystem II (PSII), have been found in plants and algae. In *Arabidopsis*, low levels of the PsbP protein led to a significant loss of the assembled PSI and PSII reaction centers (Yi et al., 2009). Similarly, previous reports have shown that R-gene-specific down-regulation of PSII transcription was observed during HR in soybeans (Glycine max) and physical damage to the reaction centers resulted in decreased photosynthetic activity (Zou et al., 2005; Jones et al., 2006). It is conceivable that these photosystem proteins are associated with oxidative burst which is the basis of plant programmed cell death, an integral part of plant defense. RuBisCO is an enzyme involved in the Calvin cycle and catalyzes the first major step in carbon fixation. The content of RuBisCO affects photorespiration which is generally associated with ROS and plant defense (Farinati et al., 2011). It was reported that the expression of vacuolar invertase in *Arabidopsis* is changed in response to T3S effector of *Pseudomonas syringae* (Bonfig et al., 2006). Furthermore, our results show that XopXccN can suppress the ROS generation in host plants (Figure 4). ROS generation in the plastoquinone pool and the possible formation of hydroperoxides in the vicinity of PSII are key processes in the primary stages of redox signaling (Ivanov and Khorobrykh, 2003). Plant defense responses include the synthesis of ROS in guard cells, cell wall crosslinking, reactions that involve peroxidases, and regulation of stomatal movement in ABA signaling (Apel and Hirt, 2004; Melotto et al., 2008; Jannat et al., 2011). Collectively, our data suggest that XopXccN contributes to the virulence of *Xcc* most if not all by suppressing ROS generation and cell wall–based defense, and interfering host photosystems.

ACKNOWLEDGEMENT

This work was supported by the Natural Science Foundation of China (30970085 and 30870071). and National Special Grant for Transgenic Researches (2009ZX08009-038B).

REFERENCES

Apel K, Hirt H (2004). Reactive oxygen species: metabolism, oxidative stress, and signal transduction. Annu. Rev. Plant. Biol., 55: 373-399.

Bonfig KB, Schreiber U, Gabler A, Roitsch T, Berger S (2006). Infection with virulent and avirulent *P. syringae* strains differentially affects photosynthesis and sink metabolism in *Arabidopsis* leaves. Planta, 225: 1-12.

Büttner D, Bonas U (2006). Who comes first? How plant pathogenic bacteria orchestrate type III secretion. Curr. Opin. Microbiol., 9: 193-200.

Büttner D, He SY (2009). Type III protein secretion in plant pathogenic bacteria. Plant Physiol., 150: 1656-1664.

Castañeda A, Reddy J, El-Yacoubi B, Gabriel D (2005). Mutagenesis of all eight *avr* genes in *Xanthomonas campestris* pv. *campestris* had no detected effect on pathogenicity, but one *avr* gene affected race specificity. Mol. Plant-Microbe Interact., 18: 1306-1317.

Corpas FJ, Barroso JB, del Rio LA (2001). Peroxisomes as a source of reactive oxygen species and nitric oxide signal molecules in plant cells. Trends Plant Sci., 6: 145-150.

Daniels M, Barber C, Turner P, Sawczyc M, Byrde R, Fielding A (1984). Cloning of genes involved in pathogenicity of *Xanthomonas campestris* pv. *campestris* using the broad host range cosmid pLAFR1. EMBO J., 3: 3323-3328.

DebRoy S, Thilmony R, Kwack YB, Nomura K, He SY (2004). A family of conserved bacterial effectors inhibits salicylic acid-mediated basal immunity and promotes disease necrosis in plants. Proc. Natl. Acad. Sci. U S A, 101: 9927-9932.

Farinati S, DalCrso G, Panigati M, Furini A (2011). Interaction between selected bacterial strains and *Arabidopsis halleri* modulates shoot proteome and cadmium and zinc accumulation. J. Exp. Bot., 62: 3433-3447.

Isaacson T, Damasceno CMB, Saravanan RS, He Y, Carmen Catalá, Saladié M, Rose JKC (2006). Sample extraction techniques for enhanced proteomic analysis of plant tissues. Nature protoc., 1: 769-774.

Ivanov B, Khorobrykh S (2003). Participation of photosynthetic electron transport in production and scavenging of reactive oxygen species. Antioxid. Redox Signal, 5: 43-53.

Jannat R, Uraji M, Morofuji M, Islam MM, Bloom RE, Nakamura Y, McClung CR, Schroeder JI, Mori IC, Murata Y (2011). Roles of intracellular hydrogen peroxide accumulation in abscisic acid signaling in *Arabidopsis* guard cells. J. Plant Physiol., 168: 1919-1926.

Jiang BL, He YQ, Cen WJ, Wei HY, Jiang GF, Jiang W, Hang XH, Feng JX, Lu GT, Tang DJ, Tang JL (2008). The type III secretion effector XopXccN of *Xanthomonas campestris* pv. *campestris* is required for full virulence. Res. Microbiol., 159: 216-220.

Jiang W, Jiang BL, Xu RQ, Huang JD, Wei HY, Jiang GF, Cen WJ, Liu J, Ge YY, Li GH, Su LL, Hang XH, Tang DJ, Lu GT, Feng JX, He YQ, Tang JL (2009). Identification of six type III effector genes with the PIP box in *Xanthomonas campestris* pv. *campestris* and five of them contribute individually to full pathogenicity. Mol. Plant-Microbe Interact., 22: 1401-1411.

Jones AM, Thomas V, Bennett MH, Mansfield J, Grant M (2006). Modifications to the *Arabidopsis* defense proteome occur prior to significant transcriptional change in response to inoculation with *Pseudomonas syringae*. Plant Physiol., 142: 1603-1620.

Kelley LA, MacCallum RM, Sternberg MJE (2000). Enhanced genome

annotation using structural profiles in the program 3D-PSSM. J. Mol. Biol., 299: 499-520.
Keshavarzi M, Soylu S, Brown I, Bonas U, Nicole M, Rossiter J, Mansfield J (2004). Basal defenses induced in pepper by lipopolysaccharides are suppressed by *Xanthomonas campestris* pv. *vesicatoria*. Mol. Plant-Microbe Interact., 17: 805-815.
Kim JG, Li X, Roden JA, Taylor KW, Aakre CD, Su B, Lalonde S, Kirik A, Chen Y, Baranage G, McLane H, Martin GB, Mudgett MB (2009). *Xanthomonas* T3S effector XopN suppresses PAMP-triggered immunity and interacts with a tomato atypical receptor-like kinase and TFT1. Plant Cell, 21: 1305-1323.
Kim JG, Taylor KW, Hotson A, Keegan M, Schmelz EA, Mudgett MB (2008). XopD SUMO protease affects host transcription, promotes pathogen growth, and delays symptom development in *xanthomonas*-infected tomato leaves. Plant Cell, 20: 1915-1929.
Lindgren PB (1997). The role of *hrp* genes during plant-bacterial interactions. Annu. Rev. Phytopathol., 35: 129-152.
Melotto M, Underwood W, He SY (2008). Role of stomata in plant innate immunity and foliar bacterial diseases. Annu. Rev. Phytopathol., 46: 101-122.
Meyer D, Lauber E, Roby D, Arlat M, Kroj T (2005). Optimization of pathogenicity assays to study the *Arabidopsis thaliana-Xanthomonas campestris* pv. *campestris* pathosystem. Mol. Plant Pathol., 6: 327-333.
Miller JH (1972). Experiments in molecular genetics. New York: Cold Spring Harbor, pp. 537-543.
Price AH, Taylor A, Ripley SJ, Griffiths A, Trewavas AJ, Knight MR (1994). Oxidative signals in tobacco increase cytosolic calcium. Plant Cell, 6: 1301-1310.
Roden JA, Belt B, Ross JB, Tachibana T, Vargas J, Mudgett MB (2004). A genetic screen to isolate type III effectors translocated into pepper cells during *Xanthomonas* infection. Proc. Natl. Acad. Sci. U S A, 101: 16624-16629.
Sambrook J, Fritsch EF, Maniatis T (1989). Molecular cloning: a laboratory manual. New York: Cold Spring Harbour Laboratory Press, pp. 76-87.
Shin R, Schachtman DP (2004). Hydrogen peroxide mediates plant root cell response to nutrient deprivation. Proc. Natl. Acad. Sci. U S A, 101: 8827-8832.
Tang DJ, Li XJ, He YQ, Feng JX, Chen B, Tang JL (2005). The zinc uptake regulator Zur is essential for the full virulence of *Xanthomonas campestris* pv. *campestris*. Mol. Plant-Microbe Interact., 18: 652-658.
Xu RQ, Blanvillain S, Feng JX, Jiang BL, Li XZ, Wei HY, Kroj T, Lauber E, Roby D, Chen B, He YQ, Lu GT, Tang DJ, Vasse J, Arlat M, Tang JL (2008). $AvrAC_{Xcc8004}$, a type III effector with a leucine-rich repeat domain from *Xanthomonas campestris* pathovar *campestris* confers avirulence in vascular tissues of *Arabidopsis thaliana* ecotype Col-0. J. Bacteriol., 190: 343-355.
Yi X, Hargett SR, Frankel LK, Bricker TM (2009). The PsbP protein, but not the PsbQ protein, is required for normal thylakoid architecture in *Arabidopsis thaliana*. FEBS Lett., 583: 2142-2147.
Zou J, Rodriguez-Zas S, Aldea M, Li M, Zhu J, Gonzalez DO, Vodkin LO, DeLucia E, Clough SJ (2005). Expression profiling soybean response to *Pseudomonas syringae* reveals new defense-related genes and rapid HR-specific downregulation of photosynthesis. Mol. Plant-Microbe Interact., 18: 1161-1174.